UCRL-90914
PREPRINT

Brightness Limitations in Multi-Kiloampere Electron Beam Sources

W. A. Barletta, J. K. Boyd,
A. C. Paul and D. S. Prono

This paper was prepared for submittal to the
1984 Free Electron Laser Conference
Villa Montecucco, Castelgandolfo, Italy
September 3 - 7, 1984

August 24, 1984

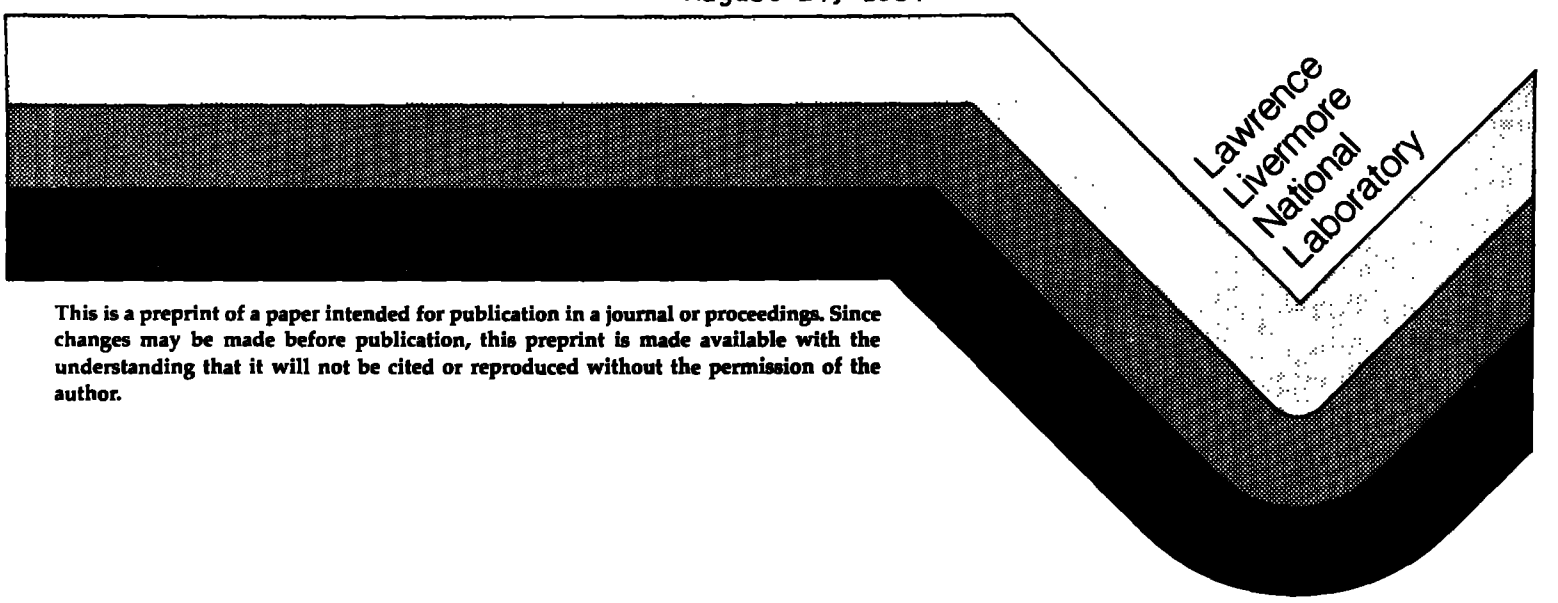

BRIGHTNESS LIMITATIONS IN MULTI-KILOAMPERE ELECTRON BEAM SOURCES

W. A. Barletta, J. K. Boyd and D. S. Prono
Lawrence Livermore National Laboratory*
Livermore, California 94550

A. C. Paul
Lawrence Berkeley Laboratory+
Berkeley, California 94720

ABSTRACT

Heuristic relationships such as the Lawson-Penner criterion, used to scale Free Electron Laser (FEL) amplifier gain and efficiency over orders of magnitude in beam current and brightness, have no fundamental basis. The brightness of a given source is set by practical design choices such as peak voltage, cathode type, gun electrode geometry, and focusing field topology. The design of low emittance, high current electron guns has received considerable attention at Livermore over the past few years. The measured brightnesses of the Experimental Test Accelerator (ETA) and Advanced Test Accelerator (ATA) guns are less than predicted with the EBQ[1] gun design code; this discrepancy is due to plasma effects from the present cold, plasma cathode in the code. The EBQ code is well suited to exploring the current limits of gridless relativistic Pierce columns with moderate current density (<50 A/cm^2) at the cathode. As EBQ uses a steady-state calculation it is not amenable for study of transient phenomena at the beam head. For this purpose, a Darwin approximation code, DPC, has been written. The main component in our experimental cathode development effort is a readily modified electron gun that will allow us to test many candidate cathode materials, types and electrode geometries at field stresses up to 1 MV/cm.

---

* Work performed jointly under the auspices of the U.S. DOE by Lawrence Livermore National Laboratory under contract W-7405-ENG-48 and for the DOD under DARPA ARPA Order No. 4395, monitored by NSWC under document N60921-84-WR-W0095.

+ This work was supported by the Director, Advanced Energy Systems, Basic Energy Sciences, Office of Energy Research, U.S. DOE under contract number DE-AC03-76SF00098.

I. INTRODUCTION

The Free Electron Laser (FEL) directly converts the energy of a relativistic electron beam to coherent radiation. In a master oscillator-power amplifier (MOPA) laser configuration, a low power input signal from a master oscillator is amplified by the electron beam in a single pass through a tapered wiggler. A multi-kiloampere, high energy, high quality electron beam is required to achieve efficient conversion of electron kinetic energy to coherent electromagnetic radiation.

Although the RF linac is well suited to drive a FEL oscillator, it does not produce enough peak current to drive a high-gain amplifier. In contrast, the linear induction accelerator can produce sufficiently bright, multi-kiloampere beams. The state-of-the-art in induction linacs is represented by the 10 kA, 50 MeV Advanced Test Accelerator (ATA) and its predecessor the Experimental Test Accelerator (ETA), both at the Lawrence Livermore National Laboratory (LLNL).

An uncertainty in predicting the output power of an FEL amplifier driven by the ATA (see Fig. 1) or ETA beam is the fraction of the beam current within a suitably small phase space volume (brightness). The input laser energy to the MOPA scales as the fifth power of the normalized beam emittance. Consequently, an optimized gun design which improved emittance by a factor as little as two or three would have an enormous impact on experimental possibilities. Conversely, for a given level of FEL performance, the required brightness scales approximately inversely with laser wavelength. As we proceed from microwave to infrared to visible wavelengths, we must build ever brighter electron beam sources perhaps sacrificing some total current capability.

II. SOURCES OF BEAM EMITTANCE

The critical importance of electron beam brightness to FEL performance has been recognized by many authors. Typically, these analyses have employed heuristic relationships such as the Lawson-Penner criterion ($I \cong 11\ E^2$ kA) to scale FEL amplifier gain and extracton over orders of magnitude in beam current. Fortunately for the MOPA approach, this scaling has no fundamental basis. The brightness of a given source is set by a variety of practical design choices such a peak voltage, cathode type, gun electrode geometry, and focusing field topology.

From a more fundamental point of view, we can identify several physical effects which can contribute to the emittance ε in a relativistic electron gun. These effects include: (1) source temperature, (2) source uniformity, (3) magnetic field normal to the cathode, (4) beam filamentation, (5) non-linear applied forces, (6) non-linear space charge forces, and (7) multiplicity or motion of emissive surfaces.

1. Source Temperature (T). The normalized source brightness, B, is related to the temperature T (eV) and source emissivity J (A/cm^2) by

$$B = \frac{jm\ (eV)}{\pi\ T\ (ev)} \simeq 1.6 \times 10^5\ J/T \quad .$$

In existing high current guns, this contribution is insignificant in comparison to other contributors to emittance. However, as we push brightnesses toward 10^6 A/cm^2-rad^2, maintaining non-emission limited sources with an effective temperature below 1 eV will be critical for cathode types with emissivity less than 10 A/cm^2.

2. Source Uniformity. To the extent that emission is non-uniform, the beam transport through regions dominated by non-linear radial forces will entrain "phase space vacuum" via phase mixing. As this dilution can become irreversible after one-quarter of a betatron wavelength, an estimate of this effect is obtained by using as the emittance the volume of the smallest ellipse enclosing all significant current regions at the cathode surface. Maintaining source uniformity argues in favor of small area cathodes with high emissivity.

3. Normal Magnetic Field. In the presence of a magnetic field normal to the cathode surface, electrons are emitted with a finite canonical angular momentum P_θ. When the electrons leave the region of axial field, they acquire a kinetic momentum sufficient to keep thier canonical angular momentum constant. This motion gives the beam an equivalent emittance in both transverse planes: $\epsilon = eB_z R^2/2\gamma\beta mc$ where B_z is the mean normal field, R is the cathode radius; $\gamma\beta$ are the usual relativistic factors; m is the electron mass; and c is the speed of light. Reducing the cathode radius reduces this contribution in two ways: (1) the emittance scales as R^2, and (2) the average value of B_z can be kept more neary zero over a smaller area.

4. Filamentation by a Grid. In gun designs with a grid, each hole in the grid can act as a focusing or defocusing lens with a focal length given by

$$1/f = e(\Delta E)/2\gamma\ \beta^2 m\ c^2$$

where ΔE is the voltage difference across the grid.

The phase space is distorted by the finite grid spacing, occurring via

filamentation downstream of the grid. Paul and Neil have described the effect[2] in the ETA gun; they report the effect to be exceeded by the effects of non-linear forces. In the design of extremely bright, high current guns, however, grid filamentation may be a limiting factor unless the grid material is extremely fine and the grid highly transparent. Unfortunately, such a grid is unlikely to be compatible with hot thermionic or dispenser cathodes, which have a low effective electron temperature. Moreover, this incompatibility will be exacerbated if the gun is operated at a repetition rate exceeding a few tens of Hertz. Moving the grid to the anode plane will minimize thermal loading and beam filamentation, but can lead to catastrophic over-focusing of multi-kiloampere beams. The most prudent choice in the design of a high brightness gun is to seek a design in which the grid has been omitted.

5. Non-linear Applied Forces. The radial forces from the applied electric and magnetic fields in guns such as the ETA and ATA injectors have significant anharmonic components (proportional to R^3). In general, these effects can be made to compensate for each other by careful design with a simulation code such as EBQ. In such simulations one must account for the other significant source of anharmonic fields, the non-linear self-fields of the beam itself.

6. Non-linear Space Charge Forces. The strong space-charge forces of an intense, low energy beam will distort the free space equipotentials to result in a defocussing spherical aberation in the beam transport. Proper shaping of the potentials by a graded accelerating column with shaped electrodes (Pierce correction) can eliminate this effect for a particular operating condition; that is, for a specified operating voltage and beam current.

Self-forces can also lead to increase in emittance whenever the beam cannot be matched into the transport. At high currents beam loading of the gun's drive circuits will lead to an energy variation correlated with time variation of the beam current. As the initial transport is space charge dominated, not all segments of the beam can be matched into the transport downstream of the injector. Phase mix damping of the mis-match oscillations will lead to an increase of beam emittance.[3]

7. Emission from Positions of Different Potentials. Even if the electrons are born with zero intrinsic temperature, the beam can acquire siginficant emittance in the extraction process if the electrons originate on different equi-potentials. Such multiple source beams have an instantaneous energy spread which will phase-mix into macroscopic emittance as the beam is accelerated and transported through the space charge dominated regime. The same consideration will limit the pulse length over which an ideal Pierce correction can be applied, if the cathode surface is a moving plasma sheath. Extraction from under-dense, moving plasmas are a worst case example of multiple, equi-potential emission.

An important tool for evaluating the relative contribution of the several souces of beam emittance is a computational model of relativistc electron beam dynamics, which can accommodate the wide range of realistic electrode geometries possible to the designer. For this purpose LLNL developed the EBQ simulation code, which was used for the design of the 10 kA ATA gun. EBQ uses a steady-state, self-consistent calculation of the particle trajectories associated with high current relativistic beam propagation in axially symmetric injectors possessing external,

two-dimensional electric and magnetic fields. The code treats the coherent electric and magnetic self-fields of the beam with sufficient accuracy in the relativistic regime, to model the high degree of cancellation which occurs between the self-magnetic and self-electric forces.

III. ADVANCED TEST ACCELERATOR INJECTOR STUDIES

Our experimental studies of brightness limitations have been done using the ATA injector (Fig. 2). This injector was not designed to maximize beam brightness; rather it was designed to produce reliably at least 10 kA with moderate brightness (10^4). Nonetheless, comparison of its performance with EBQ calculations represents our current state of understanding of beam dynamics in multi-kiloampere, repetition rated electron guns. Reconsiling the discrepancies between the calculated and measured behaviors has been the departure point for our investigations into higher brightness designs.

A. INJECTOR CHARACTERISTICS

The ATA injector consists of a plasma cathode (K) which supplies the beam electrons, an extraction control grid (G) and an anode cone (A). The 2.5 MeV accelerating potential between the cathode and anode is created by ten identical induction cores. Housed within the anode cone, over the transport beam line, are coils which focus and guide the beam. The anode voltage pulse (sum of all ten induction cores) has a ~50 ns flat top with ~30 ns rise and fall time. The control grid limits the beam extracted from the cathode to the constant portion of the anode pulse, by means of the

sharply rising grid voltage pulse (~100 kV, 8 ns rise). The grid was a 60% transparent, heavy gauge screen. The cathode surface is a plasma surface discharge[3] formed by an igniter pulse (~70 kV) which is applied at a predetermied time (τ_{ig}) relative to the extraction grid pulse. Over the 500 cm^2 cathode plane, several thousand surface breakdowns/discharges are initiated by the igniter which is resistively connected to each discharge center. These discharges quickly evolve into the cathode plasma from which electrons are extracted. Bucking coils are located behind the plasma cathode surface to cancel the B_Z from of the anode coils fringing field at the cathode plane. Operating characteristics of the injector are dependent upon the following parameters: (a) igniter timing, τ_{ig}, (b) grid voltage, V_g, (c) anode voltage, V_A, (d) cathode-grid gap, d_{K-G} (set at either 1.9 or 2.9 cm), (e) grid-anode gap, d_{G-A} (fixed at 17 cm).

In Fig. 3 we show I_k versus τ_{ig} for conditions of V_A = 2.4 MeV, d_{K-G} = 2.9 cm, V_g - 110 and 115 kV. The curve is Child-Langmuir current; i.e.,

$$I_K = APV^{3/2} (d_o - V_p \tau_{ig})^2 \quad , \tag{1}$$

where A = cathode area = 500 cm^2, P = perveance = $(4\varepsilon_o/9)(2e/m_e)^{1/2}$ = 2.33 x 10^{-6}, d_o = d_{K-g} = physical spacing from cathode plasma board surface to grid surface, v_p = expansion velocity of the cathode plasma. Normalizing the curve to the experimental data point of τ_{ig} = 80 ns, V_g = 110 kV, and I_k = 10 kA yields V_p = 10 cm/μs. With the assumption of a constant expansion velocity the predicted behavior of I_k versus $_{ig}$ clearly deviates from the data. Clearly a better model of the cathode plasma behavior is needed to fit the observed data.

Figure 4 shows the same I_k data versus the injector output I_o. Although the grid was stainless steel mesh of 60% transparency, the data show $I_i \sim 0.86\ I_K$. The focusing due to the finite wire size of grid mesh does not significantly increase the effective transparency. Reflexing of electrons (electrons reflecting between cathode surface plasma and a virtual cathode) is prevented by the grid's low transparency and hence cannot contribute to this discrepancy. These data of I_o versus I_K suggests that as much as 26% of the beam current originates on the anode side of the extractor grid.

B. BEAM EMITTANCE

Our measurements with a "pepper-pot" emittance diagnostic (Fig. 5) showed the normalized rms emittance to be roughly constant over a wide range of operating conditions. The RMS value of 0.3 - 0.4 rad-cm is two or three times larger then theoretical predictions of Paul.[5] They calculate a significant contribution to the emittance from the finite grid wire spacing. To test this sensitivity we operated the injector with two different grid materials of identical transparency but with wire spacing varied by a factor >4. Within the bounds of experimental uncertainty, the emittance of the extracted beam remained constant.

To cross-check the measurements made with the emittance box, we installed an aperture plate with a single 2 cm diameter hole on axis immediately beyond the injector. The transport beam line magnets downstream of the plate were turned off. X-ray probe scans determined the profile of the expanding beamlet at discrete axial locations. The aperture defined a

hard-edge to the beam and limited the total current to lessen the influence of space charge on beam envelope expansion. Computed beamlet profiles were fit to the measured profiles with the beam emittance as a free parameter. This procedure yields rms emittance of 0.48 rad-cm for the central beam core. Within the experimental limitations of this technique, it substantiates the emittance box measurements.

The aperture plate enabled us to confirm the importance of magnetic fields to the total beam emittance, ϵ_T, defined as $\epsilon_T^2 = \epsilon_I^2 + P_\theta^2$. Here, ϵ_I is the intrinsic emittance. The bucking coils null the leakage B_z field from the anode focus coils and thereby ensure $P_\theta = 0$. We compared the beam expansion rate with the bucking coils off and with them set to null P_θ. The injector output current monitor recorded the current and beam centroid location immediately preceding the 2 cm diameter aperture plate. Bucking coils being on or off did not affect the beam at this location. A second current monitor, located 0.7 meters downstream of the aperture recorded the transported current for bucking coils off (on) to be 1.1 (1.6) kA. In both cases the x-ray profile monitors indicated the beam was hitting the walls, expanding from the initial 1.0 cm radius to some radius, a, larger than the pipe. Thus the pipe acts as a second aperture. For emittance dominated beam expansion, the ratio of transported current as measured for bucking coils on and off $P_\theta/\epsilon_I \sim 0.7$. The magnetic field strength at the cathode without bucking coils was ~38 gauss. Projecting the ratio of current transmitted through the aperture to current incident upon the aperture as a ratio of areas, we estimate that approximately (1/7) of the 12.7 cm cathode radius was sampled. Finally, beam centroid position beyond the aperture did change for the conditions of bucking coil on/off. This variation suggests non-uniform current density being extracted from the cathode-grid region.

C. CATHODE-GRID STUDIES

Four phenomena motivated a detailed study of the plasma cathode and the control grid. The beam emerges from the injector with time varying, non-uniform current density. A sizeable fraction of the current comes from an unaccounted for source. The emittance is invariant over a wide range of operating conditions. A precursor current precedes the main current waveform; for full 10 kA operation the precursor current exceeds 1 kA for 30 ns. Furthermore, even when the main current centroid is well centered at one axial location, the precursor current centroid is far offset (>4 cm).

The scenario that emerged from this detailed study of the operating characteristics of the cathode-grid plasma and output current is as follows: the cathode discharge does not produce a well-defined plasma sheath, but rather a diffuse plasma cloud with a fast, tenuous leading edge that extends past the grid. The characteristics of this tenuous plasma are $n_p = 3.6 \times 10^9$ cm^{-3}, $T_e \sim 70$ eV, and a Debye length of 0.1 cm.

The spatial distribution of this plasma depends critically upon the igniter firing time. The plasma penetrating past the grid gives rise to a precursor current. The main grid pulse rapidly erodes this plasma, but the ions back-bombarding the grid wires release secondary electrons and cause the apparent field emisson limitations at the grid wires to be overcome. Thus, the grid becomes an extra current source of ~1.5 kA and possibly the dominant source of beam emittance. The dynamic phase (i.e., plasma erosion with density gradients, grid interaction with ion back-bombardment, and transient ion dynamics) seriously complicates the formation of the beam head and probably causes the observed poor quality of early time profiles.

More recent studies of flashboard cathode performance on a test stand, have confirmed this picture of a marginally dense plasma ($n_b \sim n_p \sim 10^{10}$ cm^{-3}) with a tenuous, fast (>40 cm/μs) component. Observations of emitted light from the cathode show considerable non-uniformities under all operating conditions, although pre-treatment of the cathode with a carbon spray ameliorates this tendency.

We conclude that flashboard sources are undesirable for high brightness beams. Grided designs appear contra-indicated for several reasons, although we have not yet ruled out such options.

IV. APPROACHES TO HIGH BRIGHTNESS

Our efforts to push the brightness of multi-kiloampere electron beams to the practical limits are proceeding along three fronts: cathode improvement, simulation and test of gridless designs, and study of transient phenomena. Candidate cathode types and injector designs are tested in the ETA and in a readily modified injector High Brightness Test Stand (HBTS).

A. CATHODE TYPES

Our survey of cathode types is limited to sources which can deliver 5 kA at >10 Hz with emissivity, $J > 5$ A/cm^2. The categories we have identified appear in Table 1. We wish to avoid cathodes that require vacuums better than 10^{-8} Torr, that are easily poisoned, or that have operating lives <500 hours. We consider maintaining source uniformity over areas exceeding a few hundred cm^2 impractical. Unless accelerating fields are extremely high

Cathode type		T_{eff}(eV)	J (A/cm^2)	B ($A/rad^2 - cm^2$)	Area (cm^2)	Vacuum (Torr)	Lifetime (hr)	Comments
Thermionic	BaO	~ 0.1	~ 5	$\lesssim 10^7$	~ 1000	10^{-7}	$< 10^3$	Moderately susceptible to poisoning
	LaB_6	~ 0.2	$\lesssim$30	$< 3 \times 10^7$	~ 200	10^{-7}	$< 10^3$	High operating temperature
Dispenser	Random porosity	~ 0.2	< 30	$< 3 \times 10^7$	~ 200	$< 5 \times 10^{-7}$	10^3	Uniformity depends on porosity
	Controlled porosity	~ 0.2	$\lesssim$40	$\lesssim 5 \times 10^7$	~ 200			Uniform, rugged
Laser heated		$\gtrsim$0.2	~ 10^3	~ 3×10^8	~ 5	10^{-8}	10^3	Easily poisoned, not mature
Photo-emissive		< 0.1	—	—	—	~ 10^{-11}	~ 10^3	
Field emission	Controlled	1	600	2×10^8	~ 10	10^{-6}	$> 10^3$	Experimental, rugged
	Uncontrolled	1	100-1000	3×10^7	~ 5 - 50			Rugged
Flashboard		~ 70	~ 30	~ 10^5	~ 200	10^{-6}	$> 10^4$	Multi-component beam

Table 1

(>1MV/cm) control of beam space charge in high J (>500 A/cm^2) designs will be difficult; hence, the source brightness in laser heated cathodes can be lost immediately. Uncontrolled field emission sources are attractive for initial experiments. Presently controlled field emitters may be useful for sources with brightness up to 10^6; however, these sources are still experimental and unavailable for early experiments. Controlled porosity, dispenser cathodes seem to offer the greatest promise for reliable operation at the limits of brightness.

B. DESIGN STUDIES

In our numerical simulations we have yet to find a multi-kiloampere injector design with a brightness limited by the cathode brightness. Gun optics and control of beam space charge dominate the emittance. Once one has chosen an extended cathode (>100 cm^2), the preferred path seems to be to find an approximation to a gridless, relativistic Pierce column. The requirement in a Pierce column is that the electrons experience no net radial force. The difficulty with this approach is that external field to null the radial forces applies to a single operating condition: beam current, voltage and cathode location; moreover, even this "point" solution requires a large number of intermediate electrodes to grade and shape the field.

An idealization of this approach is illustrated in Fig. 6(a); the electron source is a flat cathode plate surrounded by an annular shroud. Field shaping is accomplished by two artifacts: (1) A sharp anode tip bunches the equipotentials as required in an ideal Pierce column. (2) The surface connecting the anode tip normal to the shroud is a Neumann boundary, forcing

the tangential electric field to vanish along the surface. Steady-state calculations with EBQ of the electron trajectories and the macroscopic brightness as a function of axial position in the gun are given in Figs. 6 (b), (c), respectively. The current limits of this approach as well as its practical realization are under investigation for experimental test on HBTS. Relaxation of either of the two characteristic features of the design degrade the brightness by an order of magnitude. Moreover, transient effects may alter these results for short pulses.

As a code benchmark we note that EBQ code simulations of the ASTRON gun reveal that the dominant contribution to emittance was the relativistic magnetic self pinch on approach to the anode foil. The calculated emittance scaled to the operating conditions of 500 Amperes at 6 MeV is 0.019 cm-mrad; the measured value was in the range of 0.01 - 0.03 cm-mrad. The ETA gun operating at 8 kA has a calculated emittance of 0.6 cm-mrad giving a brightness of a few times 10^4. This value compares favorably with observed performance.

C. TRANSIENT PHENOMENA

As the size and cost of the accelerator drives scale with the pulse energy, we may wish to restrict the pulse length to <30 ns. Depending upon cathode type and voltage gradient, transient phenomena could shorten the amount of useful (high brightness) pulse. As it is a steady state code, EBQ is not suitable for studying phenomena at the beam head such as current bunching due to plasma shielding of the emitting surfaces. For this purpose, an axi-symmetric, particle-in-cell, Darwin approximation code, DPC, is under development.

The Darwin approximation[6] neglects the solenoidal part of the electric field in Ampere's law, transforming Maxwell's equations to elliptic form in the Coulomb gauge. Inductive effects are retained without the necessity to solve for electromagnetic waves. The electric potential is correct to all orders in v/c, and the magnetic vector potential is formally correct to order $(v/c)^2$ inclusive. The Darwin approximation reduces to solving for the magnetic vector potential using an un-retarded current. Consequently, the time step in a simulation like DPC can exceed the light speed transit time of a mesh cell. Therefore, transient effects can be studied with DPC using far fewer time steps than a full electromagnetic particle code. Presently, DPC has the capability of external magnetic field coils, finite electrode voltage rise times, and "staircase" shaping of electrodes for geometric effects.

D. EXPERIMENTAL STUDIES

Central to our experimental studies a readily modified 2 MV, several kA electron gun HBTS that will allow us to test candidate cathode materials, types and electrode geometries. The HBTS is designed to accommodate electron sources ranging from small field emission cathodes requiring up to 1 MV/cm fields to medium area (<100 cm^2) cathodes such as thermionic or plasma sources with moderate extraction fields (~100 kV/cm). The stand allows evaluation of not only the intrinsic brightness of the cathode but also the source ruggedness, usefulness for high average power operation and lifetime.

The power drives for the HBTS are MAG-1, magnetic modulators are capable of more than 100 Hz continuous operation. The radiation shielding is a pool designed to provide 10^5 attenuation. A 15 hp pump combined with a 10^4

gallon storage tank provides for a 15 minute removal of the radiation shielding. The two halves of the injector are independently mounted on tracks in order to facilitate access to the interior for work on the electrodes. A beam transport extending into a second underground room will provide an area where a sample of the electron beam can be analyzed.

V. CONCLUSIONS

We find no practical or theoretical reasons why the brightness of multi-kiloampere guns cannot be pushed well above 10^6 $A/cm^2\text{-}rad^2$. Cathodes presently under development show promise for providing rugged, reliable beam sources of kiloampere beams at brightness as high as 10^7. At such high brightness the trade-offs between beam brightness and total current must be re-evaluated.

REFERENCES

1. A. C. Paul and V. K. Neil, "High Current Relativistic Electron Guns," Advanced in Electronics and Electron Physics, Supplement 13 C, Academic Press (1983).

2. A. C. Paul, "The EBQ Code," Lawrence Berkeley Laboratory LBL-13241 (November 1982).

3. E. P. Lee, S. S. Yu and W. A. Barletta, "Phase-Space Distortion of a Heavy Ion Beam Propagating through a Vacuum Reactor Vessel," Nucl. Fusion Vol. 21, No. 8 (1981).

4. T. J. Fessenden, "Measurement of Emittance Produced by the ATA Injector," Lawrence Livermore Laboratory UCID-19839 (1983).

5. A. C. Paul, "ATA Injector Calculations," Lawrence Livermore Laboratory UCID-19197 (1981).

6. C. G. Darwin, Phil. Mag. 39, p. 357 (1920).

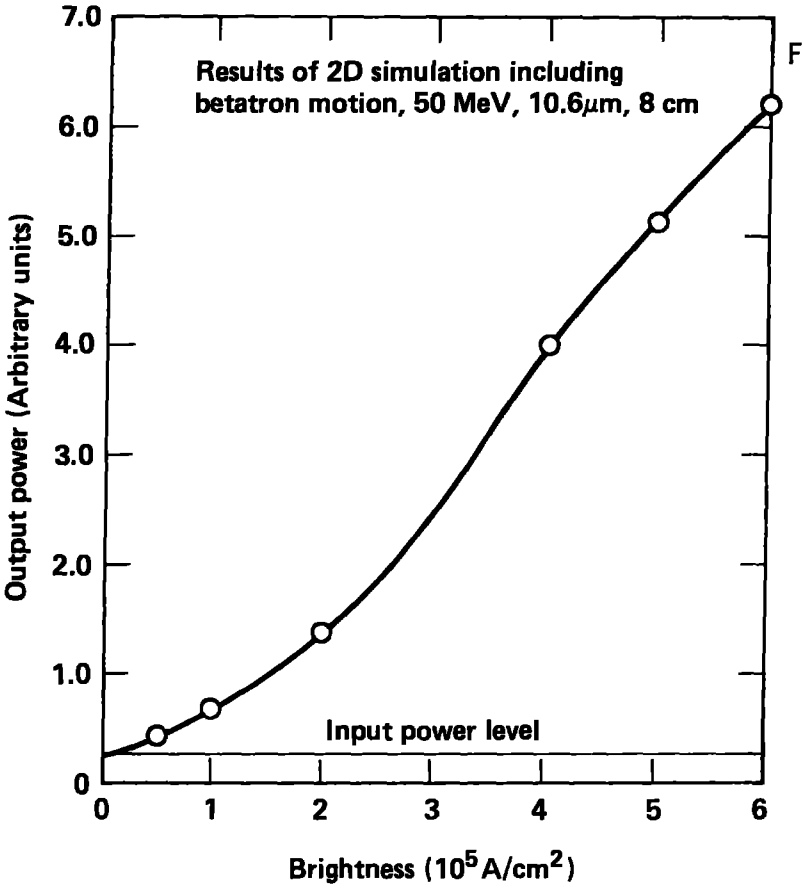

Figure 1

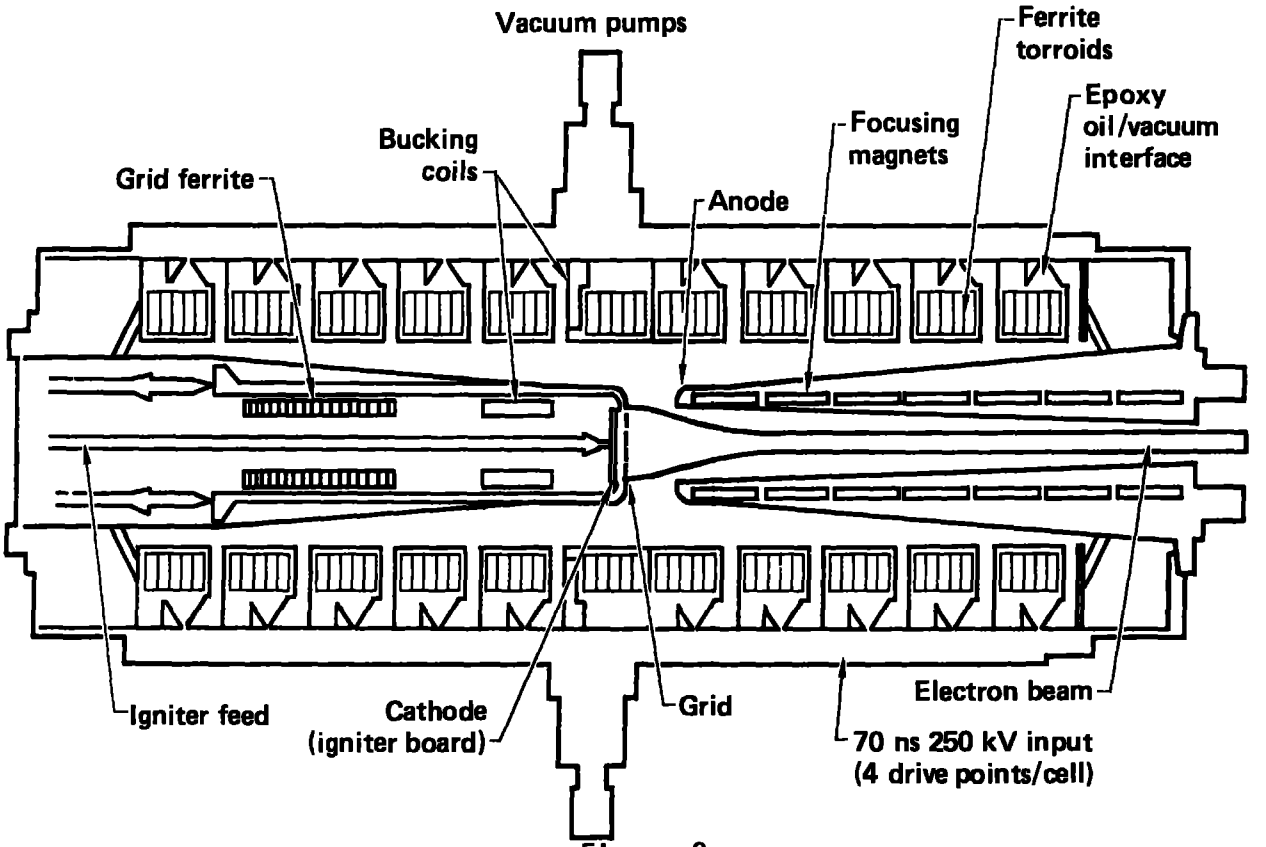

Figure 2

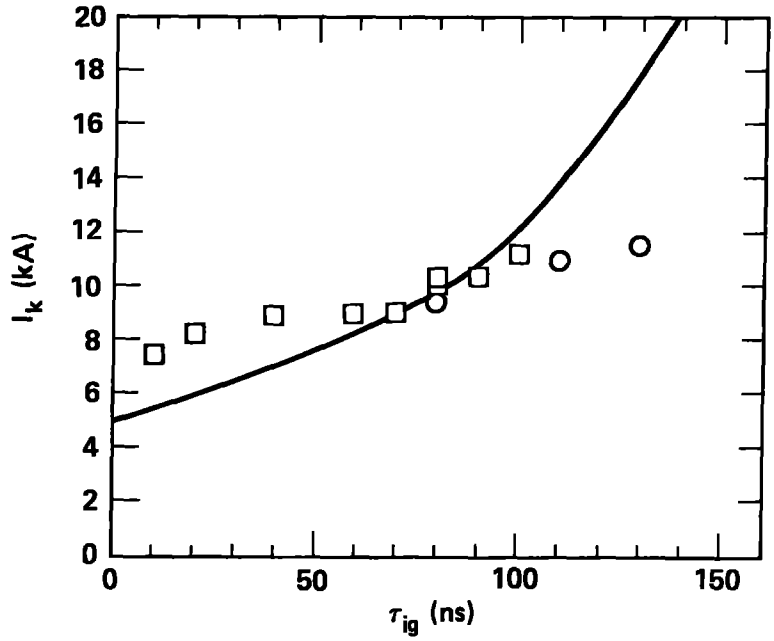

Figure 3

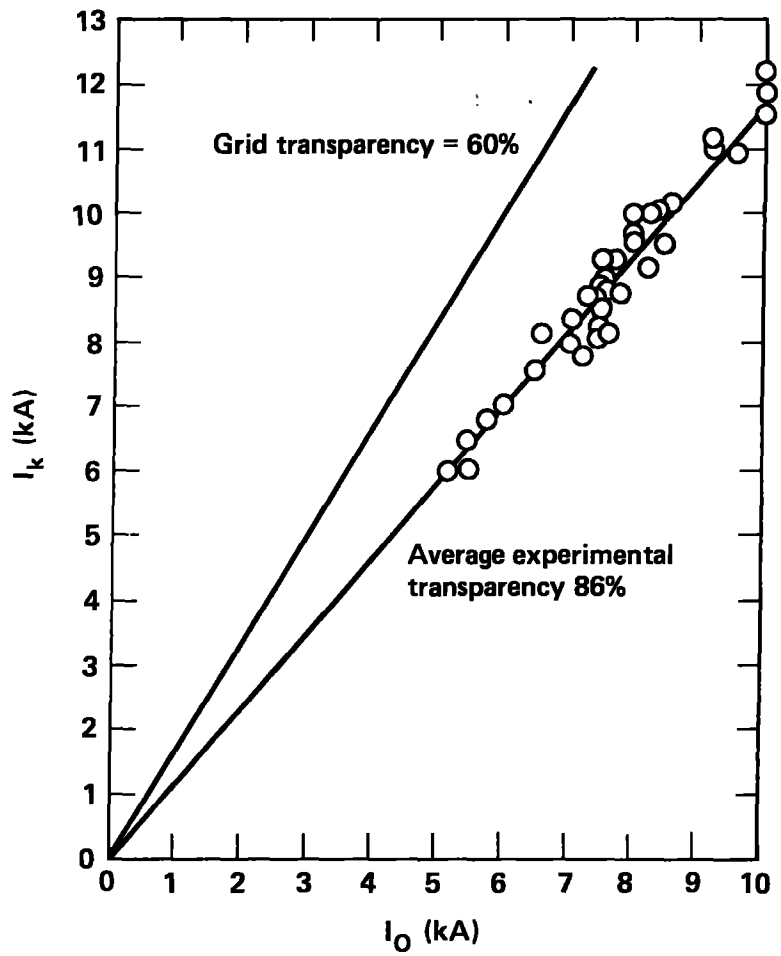

Figure 4

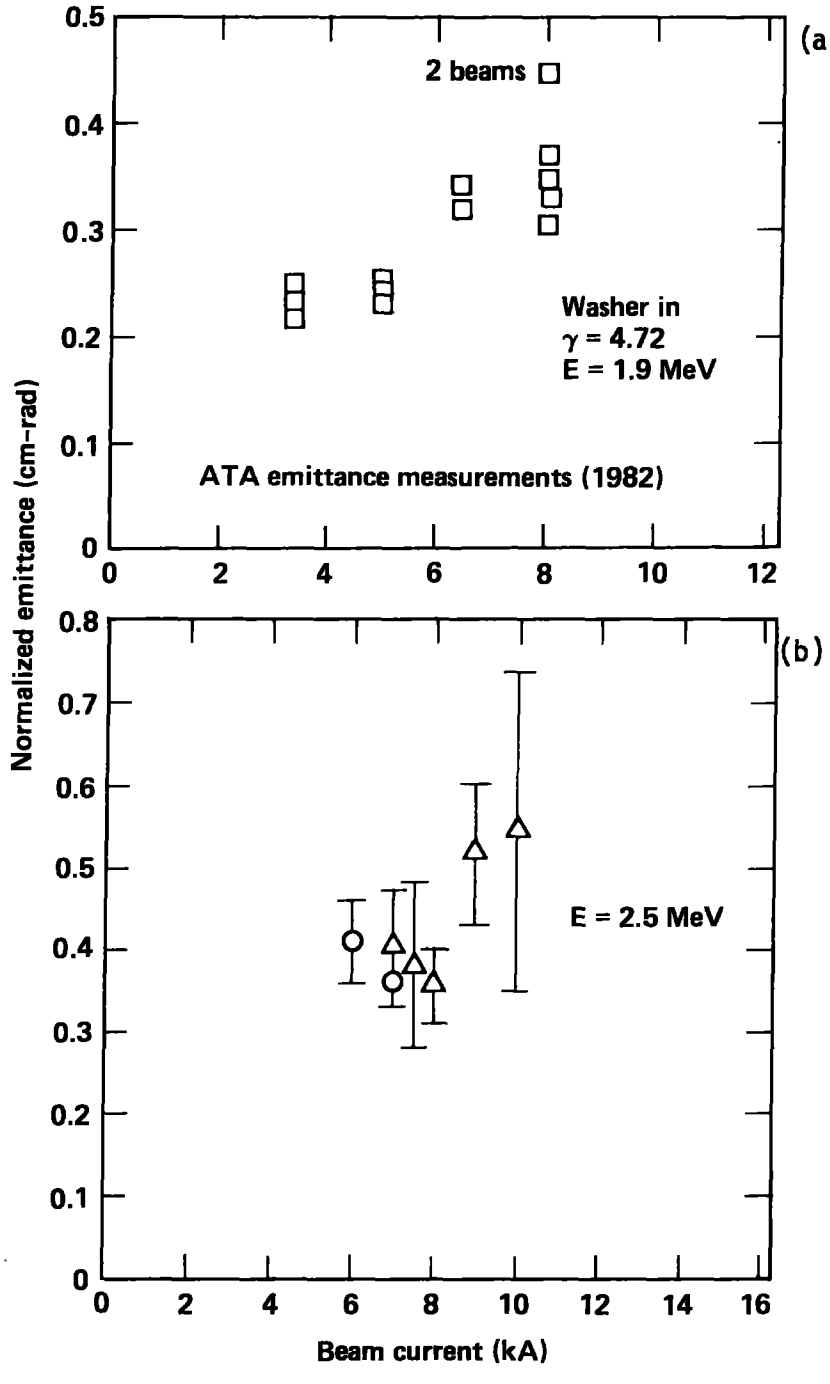
(a)
2 beams
Washer in
γ = 4.72
E = 1.9 MeV
ATA emittance measurements (1982)
(b)
E = 2.5 MeV
Normalized emittance (cm-rad)
Beam current (kA)
0.5
0.4
0.3
0.2
0.1
0
0.8
0.7
0.6
0.5
0.4
0.3
0.2
0.1
0
0 2 4 6 8 10 12
0 2 4 6 8 10 12 14 16

Figure 5

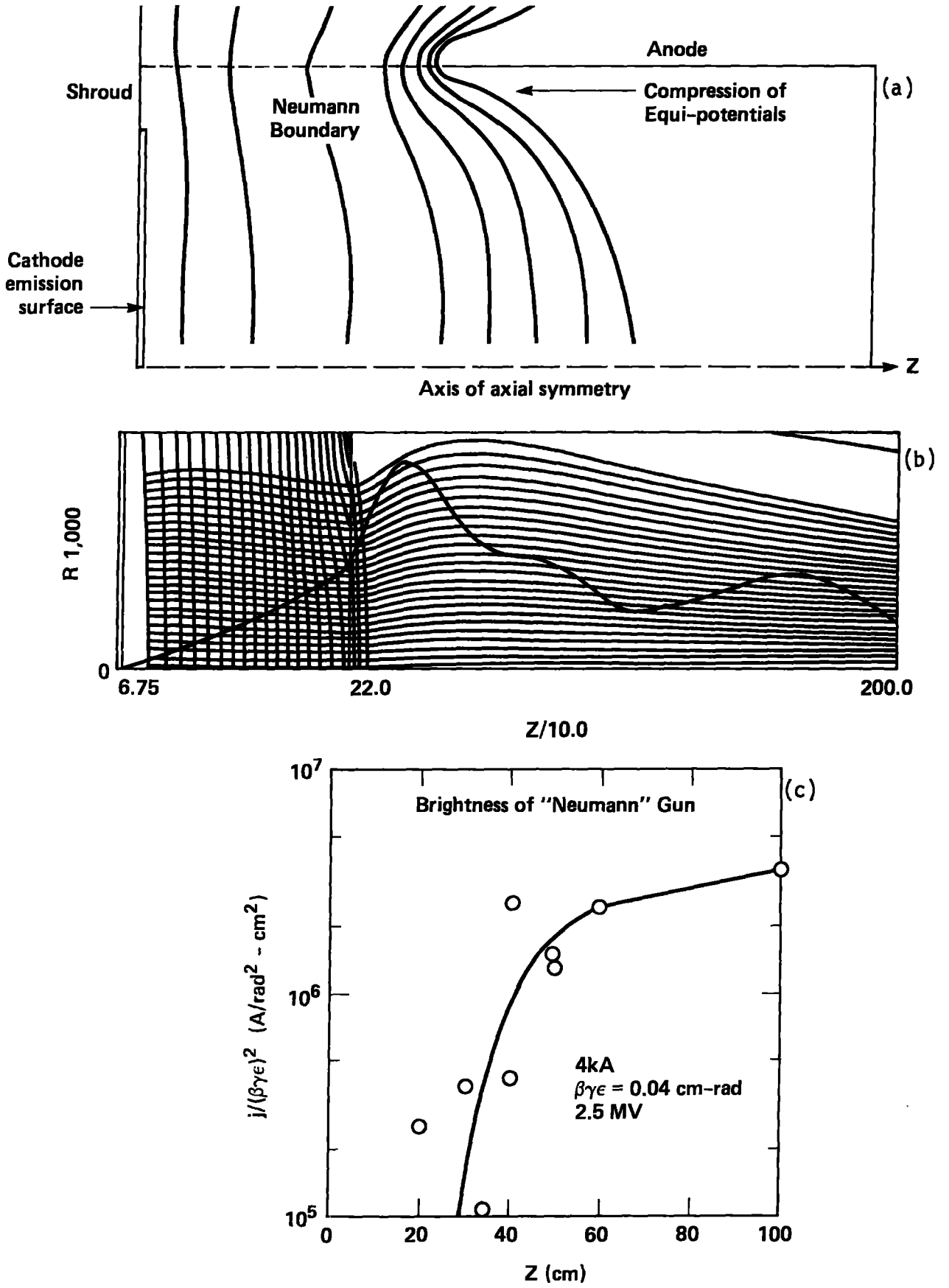
Anode
Shroud
Neumann
Boundary
Compression of
Equi-potentials
(a)
Cathode
emission
surface
Z
Axis of axial symmetry
(b)
R 1,000
0
6.75
22.0
200.0
Z/10.0
(c)
Brightness of "Neumann" Gun
10^7
10^6
10^5
$j/(\beta\gamma\epsilon)^2$ (A/rad^2 - cm^2)
4kA
$\beta\gamma\epsilon$ = 0.04 cm-rad
2.5 MV
0
20
40
60
80
100
Z (cm)

Figure 6